

Multiple pendulum and nonuniform distribution of average kinetic energy

Tetsuro Konishi*

College of Engineering, Chubu University, Kasugai 487-8501, Japan.

Tatsuo Yanagita

Department of Engineering Science, Osaka Electro-Communication University, Neyagawa 572-8530, Japan

(Dated: December 8, 2021)

Multiple pendulums are investigated numerically and analytically to clarify the nonuniformity of average kinetic energies of particles. The nonuniformity is attributed to the system having constraints and it is consistent with the generalized principle of the equipartition of energy. With the use of explicit expression for Hamiltonian of a multiple pendulum, approximate expressions for temporal and statistical average of kinetic energies are obtained, where the average energies are expressed in terms of masses of particles. In a typical case, the average kinetic energy is large for particles near the end of the pendulum and small for those near the root. Moreover, the exact analytic expressions for the average kinetic energy of the particles are obtained for a double pendulum.

I. INTRODUCTION

Pendulums are useful to explore the fundamental behavior of various physical systems. A simple pendulum is a good example of a system that can demonstrate periodic motion [1]. When the amplitude of the oscillation is small, i.e., the total energy is small, the periodic motion of a simple pendulum is well approximated by that of a harmonic oscillator, wherein the period of the oscillation does not depend on the amplitude [2].

The fundamental modes and principle of superposition can be understood by studying a double pendulum [2–5]. When the amplitude of oscillation is small, there are two special motions called the fundamental modes, wherein both the upper and lower pendulums oscillate in the same period. For a small-amplitude oscillation, one can understand that every motion of the double pendulum is expressed by the superposition of the two fundamental modes. The principle of superposition is a key concept for understanding various linear phenomena. Since both fundamental modes of the double pendulum indicates periodic motion, the double pendulum exhibits periodic or quasiperiodic motion when the amplitudes are small.

Meanwhile, a double pendulum is also a good example of a system that indicates chaotic motion [6–17]. If a large energy is assigned and the amplitudes of displacements are not small, the motion of a double pendulum is no longer regular, and chaotic behavior is observed. Multiple pendulums with three or more degrees of freedom [3–5] also exhibit chaotic behavior [18–20].

When chaos is strong in a multiple pendulum, one can expect that it admits a statistical description; the long time average of the physical quantity is considered to be approximately equal to the average over the energy surface. Then, each particle in the pendulum can be considered as a subsystem connected to a heat bath that

comprises the rest of the pendulum; then, the particles are in a thermal equilibrium.

One may expect that the system in thermal equilibrium is almost uniform. However, a careful observation of the motions of a multiple pendulum indicate that the particle at the end of the pendulum moves faster than the particle nearest to the root of the pendulum, even if the masses of all particles are the same. In fact, one author conducted numerical computations and revealed that the time average of the kinetic energies of a multiple pendulum are different [18–20]. In this paper, we revisit the observation and explain the origin of differences in the average kinetic energies using the generalized principle of the equipartition of energy [21–24]. The nonuniformity of the average kinetic energy is consistent with the generalized principle of equipartition of energy. Thus, the average kinetic energy can be nonuniform under a thermal equilibrium.

The remainder of this paper is organized as follows. In Section II, we describe our model, a multiple pendulum. Then, we provide an explicit form of the Lagrangian and Hamiltonian of a multiple pendulum. In Section III, we present the results of numerical computation where the values of time-average kinetic energies of particles in the multiple pendulum are not equal, at the same time the generalized principle of equipartition holds. In Section IV, we explain the nonuniform distribution of average kinetic energy based on statistical mechanics; further, an exact expression is obtained for the double pendulum. Finally, Section V presents the summary and the discussions.

II. MODEL

The multiple pendulum examined in this study is composed of N particles serially connected by N massless links of fixed length in a uniform gravitational field, as illustrated in Fig.1. One end is fixed to a point we define as the origin $(0, 0)$. The particles and links pass through

* e-mail: tkonishi@isc.chubu.ac.jp

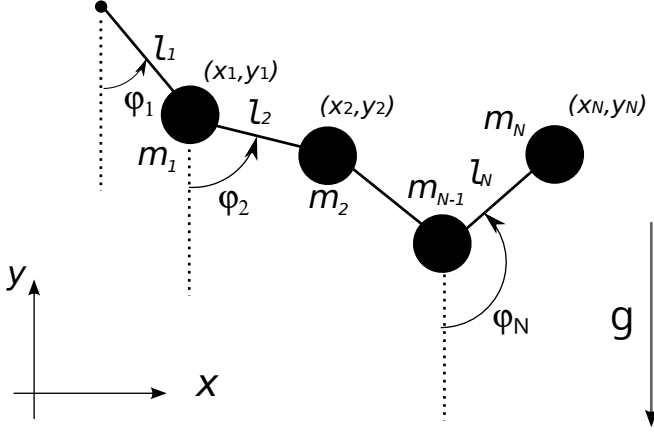


FIG. 1. Multiple pendulum: Definition of variables and parameters

each other if they arrive at the same position. The particles move in a fixed vertical plane, which is defined as the xy -plane. The x -axis is considered to be in the horizontal direction, and the y -axis, in the vertical direction with the upward direction representing the positive y direction. We let m_i , $\vec{r}_i \equiv (x_i, y_i)$, and ℓ_i represent the mass of the i 'th particle, position of the i 'th particle, and length of i 'th link, respectively. g represents the constant of gravitational acceleration. The distance between i 'th and $i+1$ 'th particles is fixed for all i . In this sense, the system has constraints.

In terms of the Cartesian coordinates (x_i, y_i) , the kinetic energy of the i 'th particle K_i , total kinetic energy K , and potential energy U are

$$K_i = \frac{m_i}{2} (\dot{x}_i^2 + \dot{y}_i^2), \quad (1)$$

$$K = \sum_{i=1}^N K_i, \quad (2)$$

$$U = \sum_{i=1}^N m_i g y_i. \quad (3)$$

Using these equations, the system is defined by a Lagrangian L and constraints G_i , which are given as

$$L = K - U = \sum_{i=1}^N \frac{m_i}{2} (\dot{x}_i^2 + \dot{y}_i^2) - \sum_{i=1}^N m_i g y_i, \quad (4)$$

$$G_i \equiv |\vec{r}_i - \vec{r}_{i-1}|^2 - \ell_i^2 = 0, \quad i = 1, 2, \dots, N, \quad (5)$$

where $\vec{r}_0 \equiv (x_0, y_0) \equiv (0, 0)$ and a dot over each symbol represents derivative with respect to time e.g., $\dot{x}_i = \frac{dx_i}{dt}$.

If we denote φ_i as the angle between the i 'th link and

the $-y$ direction (direction of gravity), we have

$$x_i = x_{i-1} + \ell_i \sin \varphi_i = \sum_{j=1}^i \ell_j \sin \varphi_j, \quad (6)$$

$$y_i = y_{i-1} - \ell_i \cos \varphi_i = - \sum_{j=1}^i \ell_j \cos \varphi_j. \quad (7)$$

The Lagrangian (4) is then expressed in terms of φ_i , $i = 1, 2, \dots, N$ as

$$L = K - U, \quad (8)$$

$$K = \sum_{i,j=1}^N \frac{1}{2} A(\varphi)_{ij} \dot{\varphi}_i \dot{\varphi}_j, \quad (9)$$

$$U = - \sum_{i=1}^N m_i g \sum_{j=1}^i \ell_j \cos \varphi_j, \quad (10)$$

where the $N \times N$ matrix A is defined as

$$A(\varphi)_{nk} \equiv \left(\sum_{i=\max(n,k)}^N m_i \right) \ell_n \ell_k \cos(\varphi_n - \varphi_k). \quad (11)$$

The derivations of Eqs. (9) and (11) are presented in Appendix A.

Using Eqs.(6) and (7), K_i can be expressed in the quadratic form of $\dot{\varphi}$ as

$$K_i = \frac{m_i}{2} \sum_{j=1}^i \sum_{k=1}^i \dot{\varphi}_j \dot{\varphi}_k \ell_j \ell_k \cos(\varphi_j - \varphi_k) \quad (12)$$

$$= \frac{1}{2} \sum_{j,k} A_{jk}^{(i)} \dot{\varphi}_j \dot{\varphi}_k \quad (13)$$

where $A^{(i)}$ represents a $N \times N$ matrix defined as

$$A_{jk}^{(i)} = \begin{cases} m_i \ell_j \ell_k \cos(\varphi_j - \varphi_k) & \dots j \leq i \text{ and } k \leq i, \\ 0 & \dots \text{otherwise.} \end{cases} \quad (14)$$

Because $\sum_i K_i = K$, the sum of $A^{(i)}$ with respect to i is equal to the matrix A :

$$\sum_{i=1}^N A_{jk}^{(i)} = A_{jk}. \quad (15)$$

Matrices A and $A^{(i)}$ depend on coordinates φ .

The momentum p_i canonically conjugate to the coordinate φ_i is defined as

$$p_i \equiv \frac{\partial L}{\partial \dot{\varphi}_i}. \quad (16)$$

Then, we have

$$p_n = \sum_{k=1}^N A_{nk} \dot{\varphi}_k, \quad (17)$$

$$K = \frac{1}{2} \sum_{j,k} p_j A_{jk}^{-1} p_k. \quad (18)$$

K_i using momentum p is expressed as

$$K_i = \frac{1}{2} \sum_{j,k,\xi,\eta} A_{jk}^{(i)} A_{j\xi}^{-1} A_{k\eta}^{-1} p_\xi p_\eta, \quad (19)$$

Using Eq.(18), the Hamiltonian of a multiple pendulum is given as

$$H = \frac{1}{2} \sum_{j,k=1}^N p_j A_{jk}^{-1} p_k - \sum_{i=1}^N m_i g \sum_{j=1}^i \ell_j \cos \varphi_j. \quad (20)$$

III. NUMERICAL EXAMPLE

A. Simulation Method

First, let us explain the methods of numerical simulation using which we integrate the equation of motion of the multiple pendulum. The equation of motion derived from the Lagrangian written in terms of φ is complicated because of the dependence of the kinetic energy on φ . Hence, we use the equation of motion written in terms of the Cartesian coordinates xy derived from Eqs.(4) and (5). The equation of motion includes the terms from the constraint characterized by the coefficients called ‘‘Lagrange multipliers’’ [2]. We numerically evaluate the Lagrange multipliers at each step of the integration to ensure that the constraints in Eq.(5) are satisfied. The idea used in this method is the same as that in the ‘‘RATTLE’’ algorithm [25–27]. We use the fourth-order symplectic integrator composed of three second-order symplectic integrators [25, 28] incorporating forces from the constraints.

We calculate the kinetic energies of the particles of the multiple pendulum. Let us denote $K_i(t)$ as the kinetic energy of the i 'th particle (Eq.(1)) at time t . The time average of $K_i(t)$ is defined as

$$\overline{K_i}(t) \equiv \frac{1}{t} \int_0^t K_i(t') dt'. \quad (21)$$

B. Simulation Results

Let us observe some typical time evolutions of the multiple pendulum obtained from the numerical simulation. Here, we adopt the initial condition $\dot{x}_i(0) = \dot{y}_i(0) = 0$ for all i ; $\varphi_i(0) = \theta$ for all i . This is a stretched configuration with angle θ .

Let us consider the initial angle as $\theta = \pi/2$. The top panel of Fig.2 shows the chaotic motion after a short transient; the bottom panel shows the temporal evolution of the average kinetic energies $\overline{K_i}(t)$. Further, $\overline{K_i}(t)$ does not converge to a single value; on the contrary, they converge to different values, i.e., the average kinetic energy is not uniform.

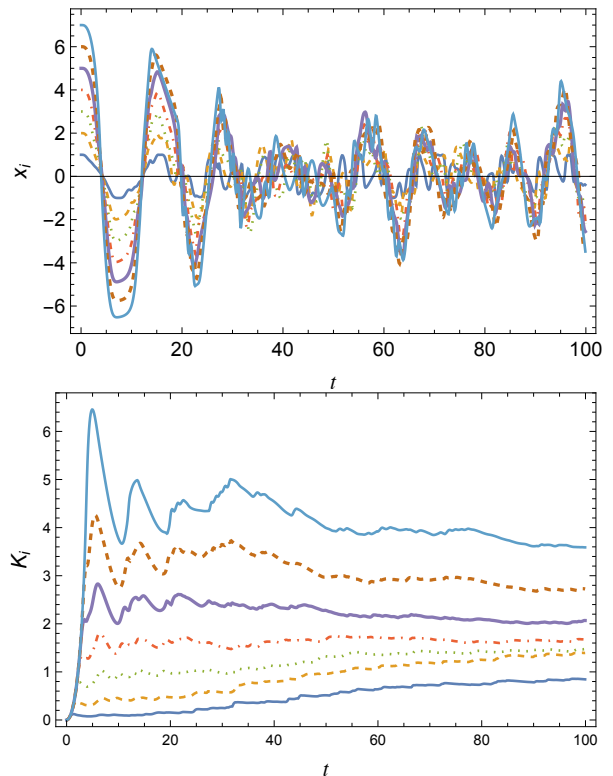


FIG. 2. (top): Time evolution of a multiple pendulum. The horizontal axis represents time, and the vertical axis represents the x coordinate of each particle $x_i(t)$. $N = 7$, $m_i = 1$, and $\ell_i = 1$ for all i ; further, $g = 1$. The time step for the numerical integration is $\Delta t = 0.001$. The initial conditions are $\varphi_i = \pi/2$ and $\dot{\varphi}_i = 0$ for all i . (bottom): Average kinetic energies $\overline{K_i}(t)$ vs. t calculated from the time evolution shown in the top panel. The lines represent $\overline{K_1}(t)$, $\overline{K_2}(t)$, \dots , and $\overline{K_7}(t)$, from the bottom to the top.

The nonuniformity in the $\overline{K_i}$ remains even if we take a longer time for averaging. Fig. 3 shows a plot of the average kinetic energy of each particle $\overline{K_i}$ (Eq.(21)) against i for $N = 16$. The values of $\overline{K_i}$ are not the same. The $\overline{K_i}$ of particles near the end are large, whereas those of particles near the root are small. This is consistent with Yanagita et al.’s first observation [18–20].

C. Non-uniformity of Average Kinetic Energy and the Generalized Principle of the Equipartition of Energy

Let us consider the relation between the non-uniformity of $\overline{K_i}$ we observed in the previous subsection and the generalized principle of the equipartition of energy [21–24].

It is natural to assume that the set of points $(\varphi_i(t), p_i(t))$, $i = 1, 2, \dots, N$ generated from the time series is close to the microcanonical ensemble because the motion of the multiple pendulum considered in this study is highly chaotic. Further, each single particle in the mul-

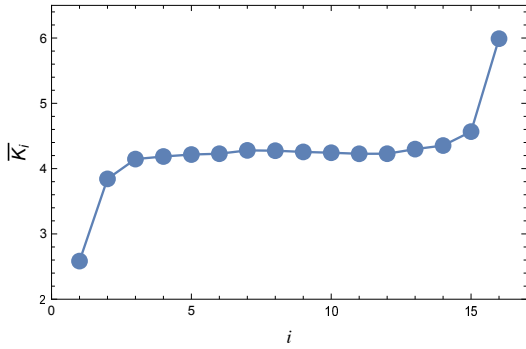


FIG. 3. Long time average of kinetic energy $\overline{K_i}(T)$ vs. i . $N = 16$, $m_i = 1$, and $\ell_i = 1$ for all i ; further, $g = 1$. The initial condition is $\varphi_i = \pi/2$, $\dot{\varphi}_i = 0$ for all i . $T = 1.0 \times 10^4$.

tiple pendulum can be regarded as a subsystem attached to a “heat bath” composed of the rest of the pendulum ($N - 1$ particles), and we can roughly approximate the statistical distribution of the state of the single particle as a canonical distribution at some temperature. This assumption allows us to interpret the original phenomena of the nonuniformity of the temporal average $\overline{K_i}$ as the nonuniformity of the thermal average $\langle K_i \rangle$. Below, we explain the nonuniformity of the thermal average using the generalized principle of the equipartition of energy.

Eq.(9) shows that the kinetic energy of the system has off-diagonal elements that depend on the coordinate φ . Thus, we cannot apply the ordinary form of the principle of the equipartition of energy. Instead, we use the generalized principle of the equipartition of energy, which states

$$\langle K_i^{(c)} \rangle = \frac{1}{2} k_B T. \quad (22)$$

Here, T represents the temperature, k_B denotes Boltzmann’s constant, the bracket $\langle \dots \rangle$ represents the thermal average, and $K_i^{(c)}$ is defined as

$$K_i^{(c)} \equiv \frac{1}{2} p_i \frac{\partial K}{\partial p_i}, \quad (23)$$

where p_i represents the momentum canonically conjugate to the coordinate φ_i . In Eq.(23), the summation with respect to i is not considered. We call K_i and $K_i^{(c)}$ the “linear kinetic energy” and “canonical kinetic energy”, respectively.

For the multiple pendulum, $K_i^{(c)}$ (Eq.(23)) is

$$K_i^{(c)} = \sum_{k=1}^N \frac{1}{2} p_i A_{ik}^{-1} p_k. \quad (24)$$

This is different from the kinetic energy of the i ’th particle K_i defined in (Eq.(19)), hence

$$K_i \neq K_i^{(c)}. \quad (25)$$

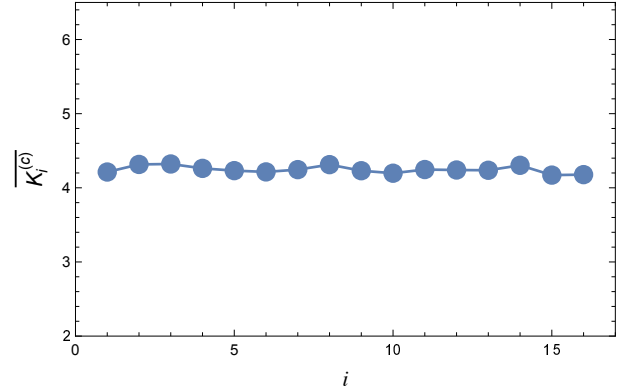


FIG. 4. Long time average of canonical kinetic energy $\overline{K_i^{(c)}}$ (Eq.(23)) vs. i . This plot was obtained using the same time series as that in Fig. 3.

Using Eqs. (22) and (25), $\langle K_i \rangle$, the average of K_i , does not take the same value at the thermal equilibrium in general.

Fig. 4 shows the time average of canonical kinetic energy Eq.(23) of the multiple pendulum using the same time series as in Fig. 3. Here, we can see that $\overline{K_i^{(c)}}$ takes almost the same value and the generalized principle of the equipartition of energy is realized. That is, even when the thermal equilibrium is established and the generalized principle of equipartition of energy holds, the average of K_i takes different values and the nonuniformity of the average kinetic energy is realized in the thermal equilibrium.

IV. ANALYTICAL EXPLANATION

A. Temporal average

If we denote

$$\Delta x_i \equiv x_i - x_{i-1}, \quad \Delta y_i \equiv y_i - y_{i-1}, \quad (26)$$

Eq.(24), the “canonical kinetic energy” of the i ’th degree of freedom, is expressed as

$$K_i^c = \sum_{j=1}^N \frac{1}{2} \left(\sum_{n=\max(i,j)}^N m_n \right) [\Delta \dot{x}_i \Delta \dot{x}_j + \Delta \dot{y}_i \Delta \dot{y}_j]. \quad (27)$$

where $\Delta \dot{x}_1 = \dot{x}_1$ and $\Delta \dot{y}_1 = \dot{y}_1$ because $x_0 \equiv y_0 \equiv 0$. Detail of calculation is shown in Appendix B.

Let us assume

$$\overline{\Delta \dot{x}_i \Delta \dot{x}_j} = 0, \quad \overline{\Delta \dot{y}_i \Delta \dot{y}_j} = 0 \quad (i \neq j). \quad (28)$$

This assumption implies that each link in the multiple pendulum rotates statistically independently.

Then, we have by straightforward calculation that

$$\overline{K_i^c} = \frac{1}{2} \left(\sum_{n=i}^N m_n \right) \left[\left(\overline{\dot{x}_i^2} + \overline{\dot{y}_i^2} \right) - \left(\overline{\dot{x}_{i-1}^2} + \overline{\dot{y}_{i-1}^2} \right) \right] \quad (29)$$

$$= \left(\sum_{n=i}^N m_n \right) \left(\frac{1}{m_i} \overline{K_i} - \frac{1}{m_{i-1}} \overline{K_{i-1}} \right). \quad (30)$$

Assuming that the temporal average $\overline{K_i^c}$ is equal to the thermal average $\langle K_i^c \rangle$ and using the generalized principle of equipartition of energy [21–23] for the “canonical kinetic energy” we have $\overline{K_i^c} = \frac{1}{2} k_B T$, and the long time average of “linear kinetic energy” of the i 'th particle K_i is recursively expressed as

$$\overline{K_i} = \frac{m_i}{m_{i-1}} \overline{K_{i-1}} + \frac{m_i}{\sum_{n=i}^N m_n} \cdot \frac{1}{2} k_B T. \quad (31)$$

Since $(x_0, y_0) = (0, 0)$ and $K_0 \equiv 0$, we have

$$\overline{K_i} = m_i \left(\sum_{j=1}^i \frac{1}{\sum_{n=i}^N m_n} \right) \cdot \frac{1}{2} k_B T. \quad (32)$$

Hence, the temporal average of the kinetic energy is nonuniform.

If all masses have the same value $m_1 = m_2 = \dots = m_N$, then $\overline{K_n}$'s are explicitly expressed as

$$\overline{K_i} = \left(\sum_{j=1}^i \frac{1}{N-j+1} \right) \frac{k_B T}{2} \quad (33)$$

so that the average linear kinetic energies $\overline{K_i}$ can monotonically increase from the root to the end of the pendulum as

$$\overline{K_1} < \overline{K_2} < \dots < \overline{K_N}. \quad (34)$$

This is consistent with the numerical results shown in Fig. 3.

B. Statistical Average

The nonuniformity of the average energy can be explained using a statistical method. Suppose the system is under thermal equilibrium at temperature T . The statistical average of the linear kinetic energy K_i is then defined as

$$\langle K_i \rangle \equiv \frac{1}{Z} \int K_i e^{-\beta H} d\Gamma, \quad (35)$$

where $Z \equiv \int e^{-\beta H} d\Gamma$, $\beta \equiv 1/k_B T$, and $d\Gamma \equiv d^N p d^N \varphi$.

Using the expression for K_i ,

$$\langle K_i \rangle = \frac{m_i}{2} \sum_{j=1}^i \sum_{k=1}^i \ell_j \ell_k \langle \dot{\varphi}_j \dot{\varphi}_k \cos \varphi_{jk} \rangle, \quad (36)$$

where $\varphi_{jk} \equiv \varphi_j - \varphi_k$.

Using Eq.(19), we can express Eq.(36) in terms of the canonical momenta p_i as

$$\langle K_i \rangle = \frac{1}{2} \sum_{j,k,\xi,\eta} \langle A_{jk}^{(i)} A_{j\xi}^{-1} A_{k\eta}^{-1} p_\xi p_\eta \rangle. \quad (37)$$

Integrating by parts with respect to p yields

$$\begin{aligned} \langle K_i \rangle &= \frac{1}{2\beta} \langle \text{tr} (A^{(i)} A^{-1}) \rangle \\ &= \frac{1}{2\beta} \frac{1}{Z} \int \text{tr} (A^{(i)} A^{-1}) e^{-\beta(\frac{1}{2} p A^{-1} p + U(\varphi))} d\Gamma. \end{aligned} \quad (38)$$

Here, matrices A^{-1} and $A^{(i)}$ depend on φ .

In Eq.(39), we first perform integration with respect to p , which is a multidimensional Gaussian integral. The result is

$$\int e^{-\beta(\frac{1}{2} p A^{-1} p)} d^N p = \left(\frac{2\pi}{\beta} \right)^{N/2} \sqrt{\det A}. \quad (40)$$

Hence, we have

$$Z = \left(\frac{2\pi}{\beta} \right)^{N/2} \int \sqrt{\det A} e^{-\beta U(\varphi)} d^N \varphi, \quad (41)$$

$$\langle K_i \rangle = \frac{1}{2\beta} \frac{\int \text{tr} (A^{(i)} A^{-1}) \sqrt{\det A} e^{-\beta U(\varphi)} d^N \varphi}{\int \sqrt{\det A} e^{-\beta U(\varphi)} d^N \varphi}. \quad (42)$$

In the following, we use these equations to express $\langle K_i \rangle$ for multiple and double pendulums.

1. Multiple Pendulum with an arbitrary number of particles

Let us adopt “diagonal approximation”

$$\langle \dot{\varphi}_j \dot{\varphi}_k \cos \varphi_{jk} \rangle = 0 \text{ for } j \neq k, \quad (43)$$

and

$$\langle A_{jj}^{-1} \rangle \approx \left\langle \frac{1}{A_{jj}} \right\rangle = \frac{1}{\left(\sum_{i=j}^N m_i \right) \ell_j^2}. \quad (44)$$

These approximations assumes that each link rotates statistically independently, and we omit all non-diagonal elements of matrix A , where phase factors such as $\cos(\varphi_i - \varphi_j)$ are included.

Then, we obtain

$$\langle K_i \rangle = m_i \left(\sum_{j=1}^i \frac{1}{\sum_{n=j}^N m_n} \right) \cdot \frac{1}{2} k_B T. \quad (45)$$

This expression is equivalent to that in Eq.(32) if the thermal average on the left-hand side $\langle \dots \rangle$ is replaced by the time average $\overline{\dots}$. The details of the calculation are summarized in Appendix C.

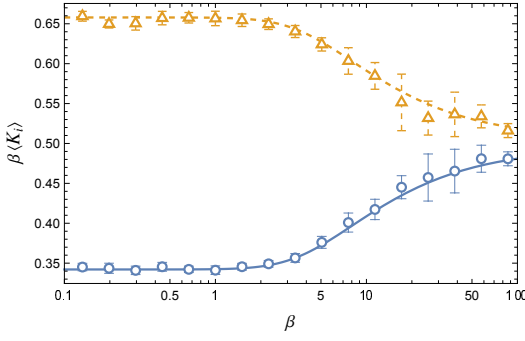


FIG. 5. β -dependence of $\langle K_i \rangle$ for double pendulum. $\beta \cdot \langle K_i \rangle$ are plotted. The upper and lower curves represent $\langle K_2 \rangle$ and $\langle K_1 \rangle$, respectively, obtained from Eqs.(57) and (56), respectively. The symbols represent the numerically obtained values of Eq.(35) using the Markov chain Monte Carlo method. $m_i = 1/2$, $\ell_i = 1$ for $i = 1, 2$. $g = 1$.

This result indicates that when all masses are the same, the average linear kinetic energies are monotonically increasing from the root to the end of the pendulum, as shown in Fig. 3.

$$\langle K_1 \rangle < \langle K_2 \rangle < \dots < \langle K_N \rangle . \quad (46)$$

2. Double pendulum

For the case of the double pendulum, i.e., for the $N = 2$ case, we can obtain the exact expressions for $\langle K_i \rangle$.

For $N = 2$, matrices A , $A^{(i)}$, defined by Eqs. (11) and (15), respectively, and $\det A$ reads

$$A = M \begin{pmatrix} \ell_1^2 & \mu_2 \ell_1 \ell_2 C_{12} \\ \mu_2 \ell_1 \ell_2 C_{12} & \mu_2 \ell_2^2 \end{pmatrix}, \quad (47)$$

$$A^{(1)} = M \mu_1 \ell_1^2 \begin{pmatrix} 1 & 0 \\ 0 & 0 \end{pmatrix}, \quad (48)$$

$$A^{(2)} = M \mu_2 \begin{pmatrix} \ell_1^2 & \ell_1 \ell_2 C_{12} \\ \ell_1 \ell_2 C_{12} & \ell_2^2 \end{pmatrix}, \quad (49)$$

$$\det A = M^2 \mu_2 \ell_1^2 \ell_2^2 (1 - \mu_2 C_{12}^2), \quad (50)$$

where

$$C_{12} = \cos(\varphi_2 - \varphi_1), \quad (51)$$

$$M = m_1 + m_2, \quad (52)$$

$$\mu_i = m_i / M. \quad (53)$$

From these, we obtain

$$\text{tr} \left(A^{(1)} A^{-1} \right) = \frac{\mu_1}{1 - \mu_2 C_{12}^2}, \quad (54)$$

$$\text{tr} \left(A^{(2)} A^{-1} \right) = \frac{(1 + \mu_2) - 2\mu_2 C_{12}^2}{1 - \mu_2 C_{12}^2} = 2 - \text{tr} \left(A^{(1)} A^{-1} \right). \quad (55)$$

Here, we used $\mu_1 + \mu_2 = 1$.

We obtain the exact expressions of $\langle K_i \rangle$ for a double pendulum by substituting these into Eq.(42) and expanding $\det A$ as a series of $\mu_2 C_{12}^2$.

$$\langle K_1 \rangle = \frac{1}{2\beta} \frac{\mu_1 \sum_{n=0}^{\infty} \frac{(2n-1)!!}{n! 2^n} \mu_2^n R_n(\alpha_1, \alpha_2)}{I_0(\alpha_1) I_0(\alpha_2) - \sum_{n=1}^{\infty} \frac{(2n-3)!!}{n! 2^n} \mu_2^n R_n(\alpha_1, \alpha_2)}, \quad (56)$$

$$\langle K_2 \rangle = \frac{1}{\beta} - \langle K_1 \rangle, \quad (57)$$

where

$$R_n(\alpha_1, \alpha_2) = \sum_{j=0}^n {}_2n C_{2j} \left\{ (2(n-j)-1)!! \right\}^2 \cdot \left\{ \frac{\partial^{2j}}{\partial \alpha_1^{2j}} \left(\frac{I_{n-j}(\alpha_1)}{\alpha_1^{n-j}} \right) \right\} \left\{ \frac{\partial^{2j}}{\partial \alpha_2^{2j}} \left(\frac{I_{n-j}(\alpha_2)}{\alpha_2^{n-j}} \right) \right\} \quad (58)$$

$$\alpha_1 = \beta(m_1 + m_2)g\ell_1, \quad (59)$$

$$\alpha_2 = \beta m_2 g \ell_2, \quad (60)$$

and $I_n(z)$ is the modified Bessel function of the n 'th order [29].

Fig. 5 shows the values of $\langle K_i \rangle$, $i = 1, 2$, calculated from Eqs.(56) and (57). We show the result of Eq.(35) obtained from Markov Chain Monte Carlo method by symbols to check the validity of Eqs.(56) and (57). We see that both calculations agree quite well.

Fig. 5 shows that $\beta \cdot \langle K_i \rangle$ appear to converge to certain finite values as $\beta \rightarrow 0$. In fact, they are calculated as

$$\lim_{\beta \rightarrow 0} \beta \cdot \langle K_1 \rangle = \frac{\mu_1}{2} \frac{K(\sqrt{\mu_2})}{E(\sqrt{\mu_2})}, \quad (61)$$

and $\lim_{\beta \rightarrow 0} \beta \cdot \langle K_2 \rangle$ is calculated from Eq.(57). Here, $K(k)$ and $E(k)$ represent the complete elliptic integrals of the 1st and 2nd kind [29], respectively. The calculation of Eq.(61) is presented in Appendix D. From this, we see that, the average kinetic energies do not depend on ℓ_i or g at the high-temperature limit. This is similar to the approximate expression in Eq.(45).

When $m_1 = m_2$, i.e., $\mu_1 = \mu_2 = 1/2$, we see that

$$\lim_{\beta \rightarrow 0} \beta \cdot \langle K_1 \rangle = 0.3431 \dots, \quad (62)$$

$$\lim_{\beta \rightarrow 0} \beta \cdot \langle K_2 \rangle = 0.6568 \dots. \quad (63)$$

These values agree well with the values obtained from the Markov Chain Monte Carlo method, as shown in Fig. 5.

Now that we have obtained the exact expression for $\langle K_i \rangle$, we can analyze their dependence on the parameters.

In Fig. 6, we show the ℓ_2 dependence of the ratio $\langle K_1 \rangle / \langle K_2 \rangle$ for $\mu_1 = 0.05, 0.5$, and 0.95 . In every case, as ℓ_2 increases, that is, the length of the lower pendulum increases, the ratio $\langle K_1 \rangle / \langle K_2 \rangle$ increases.

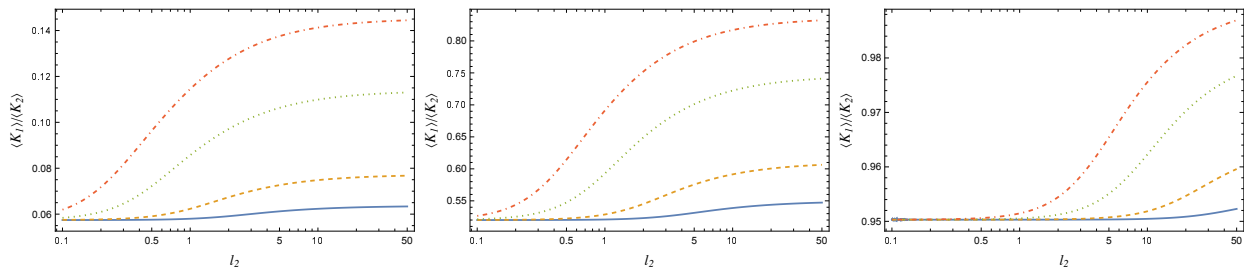


FIG. 6. l_2 dependence of the ratio $\langle K_1 \rangle / \langle K_2 \rangle$. Values of μ_1 are (left) $\mu_1 = 0.05$, (middle) $\mu_1 = 0.5$, and (right) $\mu_1 = 0.95$. Colors represent $\beta = 1, 2, 5$, and 10 from blue to red. $\ell_1 = 1$.

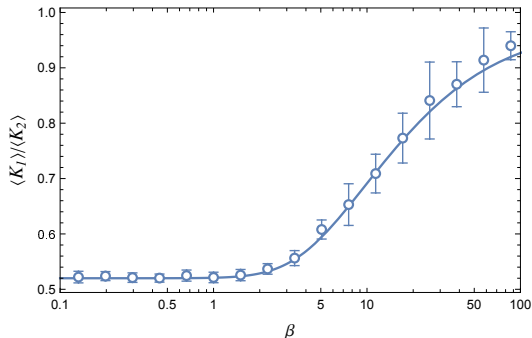


FIG. 7. β -dependence of the ratio $\langle K_1 \rangle / \langle K_2 \rangle$. The solid line represents the values obtained from Eqs.(56) and (57), and the symbols represent values obtained by the Markov Chain Monte Carlo method.

In Figure 7, we plot the β dependence of the ratio $\langle K_1 \rangle / \langle K_2 \rangle$. We see that for $\beta \rightarrow 0$, the ratio converges to a positive value, and around $\beta \sim 1$, the ratio increases gradually.

In these figures, we note two remarkable features:

- (i) At every temperature we have $\langle K_1 \rangle < \langle K_2 \rangle$. That is, the particle at the end of the pendulum has a larger average kinetic energy than the other particle near the root.
- (ii) The difference between the average kinetic energies is large for high temperatures and small for low temperatures, and a crossover temperature is observed near $\beta = 1$.

The first feature is proved as follows. From Eq.(54) and $\mu_1 + \mu_2 = 1$, we have

$$0 \leq \text{tr} \left(A^{(1)} A^{-1} \right) \leq 1 \leq \text{tr} \left(A^{(2)} A^{-1} \right) \leq 2. \quad (64)$$

Eqs.(64) and (38) indicate that

$$0 \leq \langle K_1 \rangle \leq \frac{1}{2\beta} \leq \langle K_2 \rangle \leq \frac{1}{\beta} \quad (65)$$

for any values of parameters m_i , ℓ_i , and for any temperature. Hence, the particle at the end always has a larger average kinetic energy than the other particle for a double pendulum.

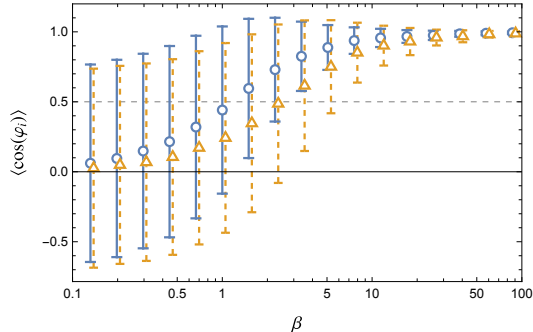


FIG. 8. β -dependence of $\langle \cos(\varphi_i) \rangle$ obtained by the Markov Chain Monte Carlo method. Open circles represent $i = 1$, and open triangles represent $i = 2$. The parameters were the same as those in Fig. 5.

Let us consider the latter feature. In Fig.8, we show $\langle \cos \varphi_i \rangle$ calculated by the Markov Chain Monte Carlo method. We observe that for high temperatures $\beta \sim 0$, $\langle \cos \varphi_i \rangle \sim 0$ for both $i = 1$ and $i = 2$. Hence, angles take various values, and the pendulum shows the rotational motion. For low temperature $\beta \gg 1$, $\langle \cos \varphi_i \rangle \sim 1$ that is, $\varphi_i \sim 0$ for both $i = 1$ and $i = 2$; the pendulum exhibits a small-angle libration. Hence, the crossover temperature observed in Fig.5 is related to crossover between the librational and rotational motions of the pendulum.

The change in the motion was observed by examining the Poincaré surface of the section of the double pendulum. Fig. 9 shows the Poincaré surface of section (φ_2, p_2) taken at $\varphi_1 = 0$ and $p_1 - p_2 \cos \varphi_2 > 0$ for several values of the total energy. As the total energy E approaches $E \sim 1$, the chaotic region in the phase space rapidly expands and fills most of the energy surface. Hence, we interpret the crossover near $\beta \sim 1$ found in previous figures as the change in motion from the limited librational to the strongly chaotic motion.

V. SUMMARY AND DISCUSSIONS

We showed that the averages of the linear kinetic energies of particles in multiple pendulum take different

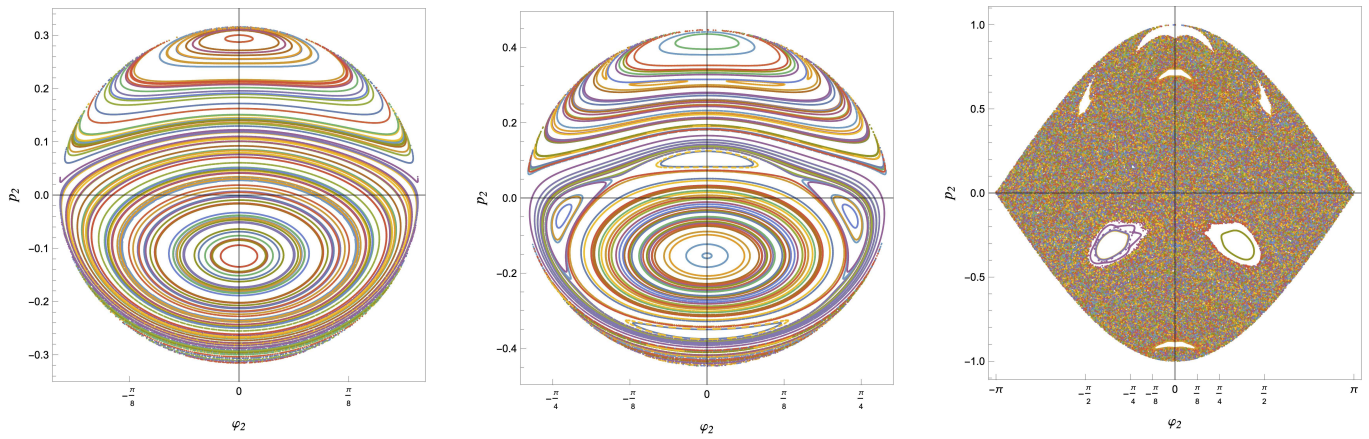


FIG. 9. Poincaré surface of section (φ_2, p_2) at $\varphi_1 = 0$, $p_1 - p_2 \cos \varphi_2 > 0$. The definition of this section is explained in the Appendix E. $m_1 = m_2 = 1$, and $\ell_1 = \ell_2 = 1$. The values of the total energy are (left) $E = 0.1$, (middle) $E = 0.2$, and (right) $E = 1.0$.

values via numerical computation and analytical calculations. Since the multiple pendulum has constraints, uniformity of average kinetic energy of each particle at thermal equilibrium is no longer guaranteed. On the contrary, another quantity what we call canonical kinetic energy is uniform, and the uniformity is guaranteed by the generalized principle of equipartition of energy. Moreover, the uniformity of the average canonical kinetic energy yields non-uniformity of the average kinetic energy of each particle.

Systems with constraints do not obey the (conventional) principle of the equipartition of energy, but a generalized one. Our discovery added a new example in which we can see how the system systematically deviates from (not generalized) equipartition [24].

The average linear kinetic energy of each particle was not the same because of the difference between the linear and canonical kinetic energies. The difference comes from the fact that the kinetic energy depends on coordinates; this dependence is attributed to the existence of constraints. In short, the constraints give rise to the nonuniform distribution of the average linear kinetic energies. This scenario is similar to a chain system without a fixed root, i.e., a freely jointed chain. Freely jointed chain is a simplified model of polymers and is composed of particles connected by massless rigid links [30–39]. For a freely jointed chain, the average kinetic energy of each particle is large near both ends of the chain and small near the middle of the chain [24].

For a double pendulum, we successfully obtained the exact expressions for $\langle K_i \rangle$. They include temperature, mass of two particles, lengths of two links, and gravitational constant. Hence, the exact expression is useful to design a system that has predefined values of average kinetic energy. Exact expressions for average kinetic energies are also obtained for a three-particle two-dimensional freely jointed chain [40], where non-uniformity of the average kinetic energies is also shown.

Further, we showed that the dependence of $\beta \cdot \langle K_i \rangle$

on the mass and length of links vanishes in the high-temperature limit. The reason why $\beta \cdot \langle K_i \rangle$ does not depend on ℓ_i or g is interpreted as follows: $\langle K_i \rangle$ depends on ℓ_i or g only through coupling with β , as in Eq.(59) and (60). Hence, in the limit $\beta \rightarrow 0$, the dependence on ℓ_i or g vanishes. This independence is also observed in the approximate expression in Eq.(45). Thus, the approximation adopted to obtain Eq.(45) is similar to the high-temperature approximation.

In this paper we considered a multiple pendulum which have constraints, and the constraints are essential for non-uniformity of average kinetic energies. In real systems there are no exact constraints; constraints appearing in models are often approximations of stiff springs and hard potentials. Suppose we have a multiple spring-pendulum where the rigid links in the multiple pendulum are replaced by springs. If the potentials are sufficiently hard, there will be a large gap between timescales of swinging motion of pendulum and vibrational motion of springs. Then, according to Boltzmann-Jeans theory [41–49], the energy exchange between swinging motion of pendulum and vibrational motion of springs take quite long time, typically exponential long with respect to the spring constant. Then we have a good chance to observe the system well approximated by rigid multiple pendulum, and average kinetic energies are non-uniform for quite long time.

Particles near the end of the pendulum have large average kinetic energy, which means the energy is localized to the particles near the end of the pendulum. There are other situations where the energy is localized to the end of the rope or chain; for example, the extremely high velocity of falling rope and cracking whip [50, 51]. Whether these similar phenomena have the same dynamical origin is an interesting question.

ACKNOWLEDGMENTS

We would like to thank Mikito Toda and Yoshiyuki Y. Yamaguchi for their fruitful discussions. T. K. was supported by a Chubu University Grant (A). T.Y. acknowledges the support of the Japan Society for the Promotion of Science (JSPS) KAKENHI Grants No. 18K03471 and 21K03411.

Appendix A: Derivation of the Lagrangian and Hamiltonian of a multiple pendulum

Here, we show a detailed derivation of the Lagrangian of a multiple pendulum (Eq.(4)). To obtain a canonical momentum conjugate to the angle φ_i

$$p_i \equiv \frac{\partial L}{\partial \dot{\varphi}_i} , \quad (\text{A1})$$

we need to express L (i.e., the kinetic energy T) in terms of φ_i and $\dot{\varphi}_i$.

First, we consider that the angles φ and Cartesian coordinates x, y are related as

$$x_i = x_{i-1} + l_i \sin \varphi_i = \sum_{j=1}^i l_j \sin \varphi_j \quad (\text{A2})$$

$$y_i = y_{i-1} - l_i \cos \varphi_i = - \sum_{j=1}^i l_j \cos \varphi_j \quad (\text{A3})$$

Then, we have

$$\begin{aligned} \dot{x}_i^2 + \dot{y}_i^2 &= \left(\sum_{j=1}^i l_j \dot{\varphi}_j \cos \varphi_j \right)^2 + \left(\sum_{j=1}^i l_j \dot{\varphi}_j \sin \varphi_j \right)^2 \\ &= \sum_{j=1}^i \sum_{k=1}^i l_j l_k \dot{\varphi}_j \dot{\varphi}_k (\cos \varphi_j \cos \varphi_k + \sin \varphi_j \sin \varphi_k) \\ &= \sum_{j=1}^i \sum_{k=1}^i l_j l_k \dot{\varphi}_j \dot{\varphi}_k \cos(\varphi_j - \varphi_k) \end{aligned} \quad (\text{A4})$$

and the kinetic energy K reads

$$K = \sum_{i=1}^N \frac{m_i}{2} \sum_{j=1}^i \sum_{k=1}^i l_j l_k \dot{\varphi}_j \dot{\varphi}_k \cos(\varphi_j - \varphi_k) . \quad (\text{A5})$$

Using an identity

$$\sum_{i=1}^N \sum_{j=1}^i \sum_{k=1}^i = \sum_{j=1}^N \sum_{k=1}^N \left(\sum_{i=\max(j,k)}^N \right) , \quad (\text{A6})$$

we obtain

$$K = \frac{1}{2} \sum_{j=1}^N \sum_{k=1}^N \left(\sum_{i=\max(j,k)}^N m_i \right) l_j l_k \dot{\varphi}_j \dot{\varphi}_k \cos(\varphi_j - \varphi_k) \quad (\text{A7})$$

$$\equiv \frac{1}{2} \sum_{j=1}^N \sum_{k=1}^N A_{jk}(\varphi) \dot{\varphi}_j \dot{\varphi}_k , \quad (\text{A8})$$

where the $N \times N$ matrix $A(\varphi)$ is defined as

$$A_{jk}(\varphi) = \left(\sum_{i=\max(j,k)}^N m_i \right) l_j l_k \cos(\varphi_j - \varphi_k) . \quad (\text{A9})$$

Using Eq.(A8), the Lagrangian of the multiple pendulum is expressed in terms of the angles φ and $\dot{\varphi}$ as

$$L = \frac{1}{2} \sum_{j=1}^N \sum_{k=1}^N A_{jk}(\varphi) \dot{\varphi}_j \dot{\varphi}_k + \sum_{i=1}^N m_i g \sum_{j=1}^i l_j \cos \varphi_j , \quad (\text{A10})$$

where matrix A is defined in Eq.(A9).

The canonical momentum p_n conjugate to the angle φ_n ($n = 1, 2, \dots, N$) can be obtained using the expression of the Lagrangian (Eq.(A10)) as

$$p_n \equiv \frac{\partial L}{\partial \dot{\varphi}_n} = \sum_{k=1}^N A(\varphi)_{nk} \dot{\varphi}_k \quad (\text{A11})$$

$$K = \sum_{i,j=1}^N \frac{1}{2} A(\varphi)_{ij} \dot{\varphi}_i \dot{\varphi}_j \equiv \frac{1}{2} \dot{\varphi}^t A(\varphi) \dot{\varphi} \quad (\text{A12})$$

$$= \sum_{i,j=1}^N \frac{1}{2} (A^{-1}(\varphi))_{ij} p_i p_j . \quad (\text{A13})$$

Then, the Hamiltonian of the multiple pendulum is obtained by the standard procedure as

$$\begin{aligned} H &= \sum_{i=1}^n p_i \dot{\varphi}_i - L \\ &= \sum_{i,j=1}^N \frac{1}{2} (A^{-1}(\varphi))_{ij} p_i p_j + U(\varphi) \end{aligned} \quad (\text{A14})$$

Appendix B: “canonical kinetic energy”

Our Hamiltonian has the form

$$H = \sum_{ij} \frac{1}{2} a_{ij}(q) p_i p_j + V(q) \quad (\text{B1})$$

where q and p are generalized coordinates and their conjugate momenta, respectively.

The generalized principle of the equipartition of energy is expressed as

$$\left\langle \frac{1}{2} p_i \frac{\partial H}{\partial p_i} \right\rangle = \frac{1}{2} k_B T \quad (\text{no sum for } i) . \quad (\text{B2})$$

Here, k_B denotes the Boltzmann constant and T represents the temperature.

$K_i^{(c)}$ is defined as

$$K_i^{(c)} \equiv \frac{1}{2} p_i \frac{\partial H}{\partial p_i} \quad (\text{no sum for } i) \quad (\text{B3})$$

$K_i^{(c)}$ is not always the same as the traditional kinetic energy of the i 'th degrees of freedom

$$K_i \equiv \frac{1}{2} m_i \dot{q}_i^2 \quad (\text{no sum for } i) \quad (\text{B4})$$

because of the off-diagonal terms in the quadratic form. To clarify these distinction, we call $K_i^{(c)}$ the ‘‘canonical kinetic energy’’ and K_i the ‘‘linear kinetic energy’’ in this paper. [52]

Below, we compute the ‘‘canonical kinetic energy’’ of the general multiple pendulum.

Our Hamiltonian is of the form

$$H(q, p) = K(q, p) + V(q) \quad (\text{B5})$$

and we have for ‘‘canonical kinetic energy,’’

$$K_i^{(c)} \equiv \frac{1}{2} p_i \frac{\partial H}{\partial p_i} = \frac{1}{2} p_i \frac{\partial K}{\partial p_i} \quad (\text{no sum for } i) \quad (\text{B6})$$

$$= \frac{1}{2} p_i \frac{\partial}{\partial p_i} \sum_{j,k=1}^N \frac{1}{2} (A^{-1})_{jk} p_j p_k \quad (\text{from (A13)}) \quad (\text{B7})$$

$$= \sum_{k=1}^N \frac{1}{2} p_i (A^{-1})_{ik} p_k \quad (\text{no sum for } i) . \quad (\text{B8})$$

The sum of the ‘‘canonical kinetic energy’’ of the i 'th angle $K_i^{(c)}$ is equal to the (total) kinetic energy K , which is given as

$$K \equiv \sum_{i=1}^N \left(\frac{1}{2} p_i \sum_{k=1}^N (A^{-1})_{ik} p_k \right) = \sum_{i=1}^N K_i^{(c)} . \quad (\text{B9})$$

Now, we express $K_i^{(c)}$ in terms of φ and $\dot{\varphi}$, and then in terms of the Cartesian coordinate x, y . Using Eq.(A11),

$K_i^{(c)}$ is expressed as

$$K_i^{(c)} = \sum_{j,k=1}^N \frac{1}{2} p_i (A^{-1})_{ik} (A_{kj} \dot{\varphi}_j) \quad (\text{no sum for } i) \quad (\text{B10})$$

$$= \frac{1}{2} p_i \dot{\varphi}_i \quad (\text{B11})$$

$$= \sum_{j=1}^N \frac{1}{2} A_{ij} \dot{\varphi}_j \dot{\varphi}_i \quad (\text{B12})$$

$$= \sum_{j=1}^N \frac{1}{2} \left(\sum_{n=\max(i,j)}^N m_n \right) \ell_i \ell_j \cos(\varphi_i - \varphi_j) \dot{\varphi}_j \dot{\varphi}_i \quad (\text{B13})$$

This is the formula which represents ‘‘canonical kinetic energy’’ of the i 'th degree of freedom in terms of φ and $\dot{\varphi}$.

The Cartesian coordinates x_i and y_i express $K_i^{(c)}$. The result is

$$K_i^{(c)} = \frac{1}{2} (\dot{x}_i - \dot{x}_{i-1}) \left(\sum_{j=i}^N m_j \dot{x}_j \right) + \frac{1}{2} (\dot{y}_i - \dot{y}_{i-1}) \left(\sum_{j=i}^N m_j \dot{y}_j \right) . \quad (\text{B14})$$

As expected, this expression for ‘‘canonical kinetic energy’’ $K_i^{(c)}$ is different from the ‘‘linear’’ kinetic energy $K_i \equiv \frac{1}{2} m_i (\dot{x}_i^2 + \dot{y}_i^2)$. Although $K_i^{(c)}$ is defined from the momentum p_i , which is canonically conjugate to the (local) angle φ_i , $K_i^{(c)}$ is extended over all particles $j = 1, 2, \dots, N$, whereas K_i is localized to a particular particle i .

1. Example: Double pendulum

Setting $N = 2$ in Eq.(B14), we have the following expressions for the ‘‘canonical kinetic energy’’ of a double pendulum.

$$K_1^{(c)} = \frac{1}{2} \{ m_1 (\dot{x}_1^2 + \dot{y}_1^2) + m_2 (\dot{x}_1 \dot{x}_2 + \dot{y}_1 \dot{y}_2) \} \quad (\text{B15})$$

$$K_2^{(c)} = \frac{1}{2} m_2 \{ (\dot{x}_2^2 + \dot{y}_2^2) - (\dot{x}_1 \dot{x}_2 + \dot{y}_1 \dot{y}_2) \} \quad (\text{B16})$$

We see that

$$K_1^{(c)} \neq K_1 \equiv \frac{1}{2} m_1 (\dot{x}_1^2 + \dot{y}_1^2) , \quad (\text{B17})$$

$$K_2^{(c)} \neq K_2 \equiv \frac{1}{2} m_2 (\dot{x}_2^2 + \dot{y}_2^2) , \quad (\text{B18})$$

$$K_1^{(c)} + K_2^{(c)} = K_1 + K_2 . \quad (\text{B19})$$

Therefore, at the thermal equilibrium, we have the average kinetic energy values of each particle of a double pendulum, which is not equal to $\frac{1}{2}k_B T$.

$$\langle K_i \rangle \neq \frac{1}{2}k_B T, i = 1, 2, \quad (\text{B20})$$

$$\langle K_1 \rangle \neq \langle K_2 \rangle. \quad (\text{B21})$$

Appendix C: Calculation of $\langle K_i \rangle$ for multiple pendulum

Let us start with Eq.(36). By applying Eq.(43), we have

$$\langle K_i \rangle = \frac{m_i}{2} \sum_{j=1}^i \ell_j^2 \langle \dot{\varphi}_j^2 \rangle. \quad (\text{C1})$$

Now, let us evaluate $\langle \dot{\varphi}_j^2 \rangle$. Note that

$$\dot{\varphi}_j = \sum_{n=1}^N A_{jn}^{-1} p_n = \frac{\partial}{\partial p_j} \frac{1}{2} \sum_{in} p_i A_{in}^{-1} p_n = \frac{\partial}{\partial p_j} H \quad (\text{C2})$$

On the other hand,

$$\frac{\partial}{\partial p_j} e^{-\beta H} = -\beta \frac{\partial H}{\partial p_j} e^{-\beta H}. \quad (\text{C3})$$

Therefore,

$$\dot{\varphi}_j = \left(\frac{-1}{\beta} \right) \frac{\partial}{\partial p_j} e^{-\beta H} \quad (\text{C4})$$

and

$$\int \dot{\varphi}_j^2 e^{-\beta H} d\Gamma = \left(\frac{-1}{\beta} \right) \int \left(\sum_n A_{jn}^{-1} p_n \right) \frac{\partial}{\partial p_j} e^{-\beta H} d\Gamma. \quad (\text{C5})$$

Performing integration by parts with respect to p_j , we obtain

$$\int \left(\sum_n A_{jn}^{-1} p_n \right) \frac{\partial}{\partial p_j} e^{-\beta H} dp_j \quad (\text{C6})$$

$$= - \int A_{jj}^{-1}(\varphi) \cdot e^{-\beta H} dp_j, \quad (\text{C7})$$

where the summation over j is not considered.

Thus, we have

$$\int \dot{\varphi}_j^2 e^{-\beta H} d\Gamma = \left(\frac{1}{\beta} \right) \int A_{jj}^{-1}(\varphi) e^{-\beta H} d\Gamma, \quad (\text{C8})$$

$$\langle \dot{\varphi}_j^2 \rangle = \frac{1}{\beta} \langle A_{jj}^{-1}(\varphi) \rangle. \quad (\text{C9})$$

Let us evaluate $\langle A_{jj}^{-1}(\varphi) \rangle$. From Eq.(A9), we have

$$A_{jj}(\varphi) \equiv \left(\sum_{i=j}^N m_i \right) \ell_j^2. \quad (\text{C10})$$

Let us adopt the approximation

$$A_{jj}^{-1} \approx \frac{1}{A_{jj}} \quad (\text{C11})$$

$$= \frac{1}{\left(\sum_{i=j}^N m_i \right) \ell_j^2}. \quad (\text{C12})$$

This approximation implies that we omit all nondiagonal elements of matrix A , which include phase factors such as $\cos(\varphi_{jk})$.

Then, we have

$$\langle \dot{\varphi}_j^2 \rangle = \frac{1}{\beta} \langle A_{jj}^{-1}(\varphi) \rangle = \frac{1}{\beta} \left\langle \frac{1}{\left(\sum_{i=j}^N m_i \right) \ell_j^2} \right\rangle \quad (\text{C13})$$

$$= \frac{1}{\beta \left(\sum_{i=j}^N m_i \right) \ell_j^2}. \quad (\text{C14})$$

Therefore, we obtain

$$\langle K_i \rangle = \frac{m_i}{2} \langle \dot{x}_i^2 + \dot{y}_i^2 \rangle = \frac{m_i}{2} \sum_{j=1}^i \langle \dot{\varphi}_j^2 \rangle \ell_j^2 \quad (\text{C15})$$

$$= k_B T \cdot \frac{m_i}{2} \sum_{j=1}^i \frac{1}{\sum_{k=j}^N m_k}. \quad (\text{C16})$$

Appendix D: Calculation of $\lim_{\beta \rightarrow 0} \beta \cdot \langle K_1 \rangle$

Here, we present the calculation of Eq.(61), which represent the high-temperature limit $\lim_{\beta \rightarrow 0} \beta \cdot \langle K_1 \rangle$. From Eqs. (42), (50), and (54), we have

$$\beta \langle K_1 \rangle = \frac{\mu_1}{2} \frac{\int_{(0,2\pi)^2} \frac{1}{\sqrt{1-\mu_2 C_{12}^2}} e^{-\beta U(\varphi)} d^2 \varphi}{\int_{(0,2\pi)^2} \sqrt{1-\mu_2 C_{12}^2} e^{-\beta U(\varphi)} d^2 \varphi} \quad (\text{D1})$$

for the double pendulum. Here, $C_{12} = \cos(\varphi_2 - \varphi_1)$. Considering the limit $\beta \rightarrow 0$ on both sides, we have

$$\begin{aligned} \lim_{\beta \rightarrow 0} \beta \cdot \langle K_1 \rangle &= \frac{\mu_1}{2} \frac{\int_{(0,2\pi)^2} \frac{1}{\sqrt{1-\mu_2 C_{12}^2}} d^2 \varphi}{\int_{(0,2\pi)^2} \sqrt{1-\mu_2 C_{12}^2} d^2 \varphi} \\ &= \frac{\mu_1}{2} \frac{K(\sqrt{\mu_2})}{E(\sqrt{\mu_2})}, \end{aligned} \quad (\text{D2})$$

where $K(k)$ and $E(k)$ are the complete elliptic integrals of the 1st and 2nd kind, respectively.

Appendix E: Poincaré surface of section

Here, we explain the definition of the Poincaré surface of the section used in Fig. 9. A unique correspondence from a point (φ_2, p_2) on the surface to a single point $(\varphi_1, \varphi_2, p_1, p_2)$, in the phase space is necessary. We set

two conditions $H(\varphi, p) = E$ and $\varphi_1 = 0$, which reduces the four-dimensional phase space to a two-dimensional space (φ_2, p_2) . Let us specify a point (φ_2, p_2) on the Poincaré surface.

For systems including a double pendulum, the energy is of the form

$$\frac{1}{2}pA^{-1}p + U(\varphi_1, \varphi_2) = E. \quad (\text{E1})$$

Let us express matrix A as

$$A = \begin{pmatrix} A_1 & A_2 \\ A_2 & A_3 \end{pmatrix}. \quad (\text{E2})$$

By substituting this into Eq.(E1) and the straightforward calculation, we get

$$(A_3p_1 - A_2p_2)^2 = \det A \{2A_3(E - U(\varphi_1, \varphi_2)) - p_2^2\} \quad (\text{E3})$$

Hence, point (φ_2, p_2) corresponds to a unique point $(\varphi_1, \varphi_2, p_1, p_2)$ under $E = \text{const}$, and we must specify the sign of $A_3p_1 - A_2p_2$. Let us take a positive sign; then, the Poincaré surface of the section is defined as

$$\begin{cases} \varphi_1 & = 0, \\ A_3p_1 - A_2p_2 & > 0. \end{cases} \quad (\text{E4})$$

In the case of a double pendulum, the last condition is equivalent to

$$\mu_2\ell_2^2p_1 - \mu_2\ell_1\ell_2p_2 \cos \varphi_2 > 0. \quad (\text{E5})$$

by substituting $\varphi_1 = 0$. For $\ell_1 = \ell_2$, this condition yields

$$p_1 - p_2 \cos \varphi_2 > 0, \quad (\text{E6})$$

as shown in Fig. 9.

Using

$$\dot{\varphi} = A^{-1}p, \quad (\text{E7})$$

we can convert the condition in Eq.(E4) in terms of $\dot{\varphi}$. Since

$$A_3p_1 - A_2p_2 = \dot{\varphi}_1 \cdot \det A, \quad (\text{E8})$$

and the kinetic energy and matrix A are positive definite, we can consider

$$\varphi_1 = 0, \quad \dot{\varphi}_1 > 0 \quad (\text{E9})$$

as the surface of the section.

-
- [1] G. Galilei, *Dialogues Concerning Two New Sciences* (Lodewijk Elzevir, 1638).
- [2] H. Goldstein, *Classical Mechanics, 2nd ed.* (Addison-Wesley, 1980).
- [3] D. Bernoulli, *Commentarii Academiae Scientiarum Imperialis Petropolitanae* **6**, 108 (1738).
- [4] D. Bernoulli, *Commentarii Academiae Scientiarum Imperialis Petropolitanae* **7**, 162 (1740).
- [5] J. T. Cannon and S. Dostrovsky, *The Evolution of Dynamics: Vibration Theory from 1687 to 1742* (Springer-Verlag, 1981).
- [6] A. J. Lichtenberg and M. A. Lieberman, *Regular and Chaotic Dynamics* (Springer, 1992).
- [7] E. Ott, *Chaos in Dynamical Systems, 2nd.ed.* (Cambridge University Press, Cambridge, 2002).
- [8] M. Tabor, *Chaos and Integrability in Nonlinear Dynamics: An Introduction* (Wiley Interscience, 1989).
- [9] T. Shinbrot, C. Grebogi, J. Wisdom, and J. A. Yorke, *American Journal of Physics* **60**, 491 (1992).
- [10] T. Stachowiak and T. Okada, *Chaos, Solitons & Fractals* **29**, 417 (2006).
- [11] M. Z. Rafat, M. S. Wheatland, and T. R. Bedding, *American Journal of Physics* **77**, 216 (2009).
- [12] H. R. Dullin, *Zeitschrift für Physik B Condensed Matter* **93**, 321 (1994).
- [13] T. Stachowiak and W. Szumiński, *Physics Letters A* **379**, 3017 (2015).
- [14] A. V. Ivanov, *Regular and Chaotic Dynamics* **4**, 104 (1999).
- [15] A. V. Ivanov, *Journal of Physics A: Mathematical and General* **34**, 111011 (2001).
- [16] A. V. Ivanov, *Regular and Chaotic Dynamics* **5**, 329 (2000).
- [17] A. V. Ivanov, *Regular and Chaotic Dynamics* **6**, 53 (2001).
- [18] Y. Oyama and T. Yanagita, (1998), talk at The Autumn Meeting of The Physical Society of Japan, 25a-G-6.
- [19] N. Saitoh, Y. Oyama, and T. Yanagita, (1999), talk at The Annual Meeting of The Physical Society of Japan, 30p-XD-5.
- [20] N. Saitoh and T. Yanagita, (2000), talk at The Spring Meeting of the Physical Society of Japan, 23aZB-6.
- [21] R. C. Tolman, *Physical Review* **11**, 261 (1918).
- [22] R. C. Tolman, *The Principles of Statistical Mechanics* (Oxford University Press, Oxford, 1938).
- [23] R. Kubo, H. Ichimura, T. Usui, and N. Hashitsume, *Statistical Mechanics* (North Holland, 1990).
- [24] T. Konishi and T. Yanagita, *J. Stat. Mech.*, L09001 (2009).
- [25] B. Leimkuhler and S. Reich, *Simulating Hamiltonian Dynamics* (Cambridge Univ. Press, 2004).
- [26] <http://www.charmm.org/>, "CHARMM (Chemistry at HARvard Macromolecular Mechanics)."
- [27] F. J. Vesely, *American Journal of Physics* **81**, 537 (2013), <https://doi.org/10.1119/1.4803533>.
- [28] H. Yoshida, *Phys. Lett.* **150A**, 262 (1990).
- [29] "NIST Digital Library of Mathematical Functions," <https://dlmf.nist.gov/>.
- [30] W. Kuhn, *Kolloid-Zeitschrift* **68**, 2 (1934).
- [31] W. Kuhn and H. Kuhn, *Journal of Colloid Science* **3**, 11 (1948).
- [32] H. A. Kramers, *J. Chem. Phys.* **14**, 415 (1946).
- [33] M. Fixman, *Proceedings of the National Academy of Sciences* **71**, 3044 (1974).
- [34] M. Fixman and J. Kovac, *The Journal of Chemical Physics* **61**, 4950 (1974).
- [35] M. Mazars, *Phys. Rev. E* **53**, 6297 (1996).
- [36] M. Doi and S. Edwards, *The theory of polymer dynamics*

- (Clarendon Press, Oxford, 1988).
- [37] M. Doi, *Introduction to Polymer Physics* (Oxford University Press, Oxford, 1996).
- [38] G. R. Strobl, *The Physics of Polymers: Concepts for Understanding Their Structures and Behavior* (Springer, 1997).
- [39] G. R. Siegert, R. G. Winkler, and P. Reineker, *Zeitschrift für Naturforschung A* **48**, 584 (1993).
- [40] T. Konishi and T. Yanagita, in preparation.
- [41] L. Boltzmann, *Nature* **51**, 413 (1895).
- [42] J. H. Jeans, *Phil. Mag.* **6**, 279 (1903).
- [43] J. H. Jeans, *Phil. Mag.* **10**, 91 (1905).
- [44] N. Nakagawa and K. Kaneko, *Phys. Rev. E* **64**, 055205 (2001).
- [45] G. Benettin, L. Galgani, and A. Giorgilli, *Physics Letters A* **120**, 23 (1987).
- [46] G. Benettin, L. Galgani, and A. Giorgilli, *Comm. Math. Phys.* **121**, 557 (1989).
- [47] G. Benettin, *Prog. Theor. Phys. Suppl.* **116**, 207 (1994).
- [48] T. Konishi and T. Yanagita, *J. Stat. Mech.* , P09001 (2010).
- [49] T. Konishi and T. Yanagita, *J. Stat. Mech.* , 033201 (2016).
- [50] A. Goriely and T. McMillen, *Phys. Rev. Lett.* **88**, 244301 (2002).
- [51] W. Tomaszewski and P. Pieranski, *New Journal of Physics* **7**, 45 (2005).
- [52] The term “linear” is used because the “momentum” $m\dot{q}$ is often called as the “linear momentum”.